Nd:YAG Laser Beam Welding of Coated Steels Using a Modified Lap Joint Geometry

Nd:YAG laser beam welding of galvanized and galvannealed sheet steels in the lap-joint configuration is made possible using a modified joint geometry

BY M. P. GRAHAM, D. C. WECKMAN, H. W. KERR, AND D. M. HIRAK

ABSTRACT. The weldability of coated sheet steels by Nd:YAG lasers has been examined using a 250-W pulsed laser, a 1-kW pulsed laser and a 2-kW continuous wave (CW) laser. Seam welds were produced in 0.75-mm-thick (23- gauge) galvanized and galvannealed sheet steels using a modified lap-joint configuration consisting of a groove-shaped projection in the top sheet of the joint. Experiments were performed to assess the effects on weld quality of coating type, groove-projection dimensions and laser process parameters.

Good quality welds, which failed at levels comparable to the base metal in shear tensile tests, were made over a wide range of conditions using the CW Nd:YAG laser, but could only be produced using a limited range of process conditions with the two pulsed lasers. Using the CW laser at a mean power of 1600 W, good quality welds could be produced at speeds up to 60 mm/s (144 in./min). In comparison, the maximum acceptable welding speed when using the 250-W pulsed laser at 220 W laser mean power was just 2.4 mm/s (5.4 in./min). The melting ratios of the welds produced with the CW laser were found to be about 0.25, while they were approximately 0.10 for the welds produced using the pulsed lasers. Finally, the quality of welds produced was not affected by the dimensions of the groove projection or by the coating type.

M. P. GRAHAM, D. C. WECKMAN, and H. W. KERR, are with the Department of Mechanical Engineering, University of Waterloo, Waterloo, Ontario, Canada. D. M. HIRAK is with Imperial Oil Resources. Ltd, Calgary, Alberta, Canada.

Introduction

The automotive industry uses zinc-rich coated sheet steels extensively in auto body components for enhanced corrosion resistance. Laser beam welding is being evaluated as an alternative joining technique for these sheet steels in the lap-joint configuration, because it offers a number of advantages over traditional resistance spot welding practices. For example, much less flange material is required for laser welding, resulting in a potentially significant weight reduction. As well, no direct contact is required between the welding machine and the workpiece and access is only required from one side of the weld joint. In addition, lasers, particularly Nd:YAG lasers whose output can be transmitted through fiber-optic cables, can be easily integrated into automotive robotic welding cells.

Laser beam welding of zinc-coated sheet steel in the lap-joint configuration is illustrated schematically in Fig. 1A. The well-known problem with welding these materials in this configuration is related to the low boiling point of zinc

KEY WORDS

Nd:YAG
Laser Beam Welding
Lap-Joint Configuration
Galvanized Sheet Steels
Coated Sheet Steels
Joint Design
Automotive Welding

(906°C/1663°F) compared with the melting temperature of steel (~1550°C/2822°F). During seam welding, the two zinc coatings at the interface vaporize and expand rapidly when the molten steel weld pool approaches the interface between the two steel sheets. With no joint clearance between the sheets, this vapor can only escape through the molten weld pool, and this typically results in excessive weld porosity or complete expulsion of the weld metal.

Many different techniques have been attempted to allow production of acceptable seam welds in the lap-joint configuration in coated sheet steels using both CO_2 and Nd:YAG lasers and no joint clearance between the two sheets of steel. The use of CO_2 and Nd:YAG lasers pulsed at different frequencies has been reported to permit the production of good quality, full joint penetration welds with no joint clearance (Refs. 1–7). Unfortunately, acceptable welds have only been created using a small window of processing conditions and these conditions have been found to be affected by a number of process parameters including the coating type and thickness, the sheet thickness, the laser power and the type of laser. The effects of pulsing of the beam on the welding process are not yet fully understood.

In a recent study, the weldability of laser beam welding coated sheet steels in a lap-joint configuration with no clearance between the sheets was examined using a 2-kW Nd:YAG laser capable of CW and sine or square wave modulated output (Ref. 8). The results of the study showed that good quality welds could not be produced using these lasers when there was no joint clearance between the two sheets of steel. Invariably, the welds displayed excessive porosity or complete weld metal expulsion due to the zinc vapor created at the interface between the two sheets during welding.

Good quality laser beam seam welds have been reported when the zinc coating in the area of the weld was removed prior to welding (Refs. 9, 10); however, the cost of this additional processing step may be prohibitive. Alternatively, there are a large number of laser welding techniques for laser beam welding of these coated sheet steels which have been designed to provide adequate venting of the zinc vapor from between the two sheets rather than through the weld pool. Good quality welds have been produced using continuous wave (CW) CO_2 lasers and both pulsed and CW Nd:YAG lasers, for example, by introducing a small joint clearance between the sheets using preplaced shims as shown in Fig. 1B (Refs. 11–13). It has been shown that clearances ranging from 0.04 to 0.3 mm (0.0016 to 0.01 in.), depending on the type of coating, coating thickness, etc., provide an alternate path for venting of the zinc vapor (Refs. 8, 12–15). For a particular coated sheet steel, however, good quality welds can only be produced over a narrow range of clearance sizes (on the order of 0.1 to 0.2 mm/0.004 to 0.008 in.) and the required joint clearance depends on a number of variables including coating type and thickness, sheet thickness, laser type and beam diameter, and welding speed. Although this approach has been shown to permit the production of good quality laser beam welds in a laboratory setting, the difficulty of maintaining a controlled joint clearance between the sheets has prevented rapid acceptance of a fixed-clearance technique in production environments.

Coated sheet steels have been laser welded using a number of modified lap-joint geometries, which have been designed to create a controlled joint clearance between the sheets with minimal fixturing. This has been done dynamically during welding using a roller device (Ref. 16) or by prestamping stand-off projections into the top steel sheet and welding through the clearance between the projections as shown in Fig. 1C (Refs. 17–19). The difficulty with these techniques remains that the required joint clearance is still within a narrow range of dimensions and is sensitive to variations of many of the process parameters, as described above.

In the present study, a new joint geometry for laser welding of these coated materials in a lap-joint configuration was developed and evaluated. The geometry consists of a rounded groove-shaped projection pressed into the top sheet of the lap-joint specimen pair, as shown in Fig. 2. This technique differs from the previously reported techniques involving preformed projections as described above in that the weld is made along the point of contact between the two sheets rather than through the clearance created by the projection. The advantage of this new joint geometry is that it allows the top and bottom sheets to be clamped firmly in contact during welding while still providing a vent path between the sheets for the zinc vapor to dissipate. It has the additional advantages that weld quality is not sensitive to dimensional variations of the joint clearance formed between the sheets and that the groove can be followed easily by a real-time joint tracker.

The objective of the work reported here was to evaluate the weldability of galvanized and galvannealed sheet steels with the grooved-projection lap-joint configuration using three Nd:YAG lasers; a 250-W pulsed laser, a 1-kW pulsed laser and a 2-kW CW laser. The specific aims were to determine the possible influences on weld quality of various process parameters including output power waveform, mean laser power, welding speed, groove projection geometry and coating type.

Experimental Apparatus and Procedures

Two different coated sheet steels were used in this study: 0.75-mm-thick (23-ga) hot-dipped galvanized sheet with a minimum zinc coating of 60 g/m^2 on each side (nominal coating thick-

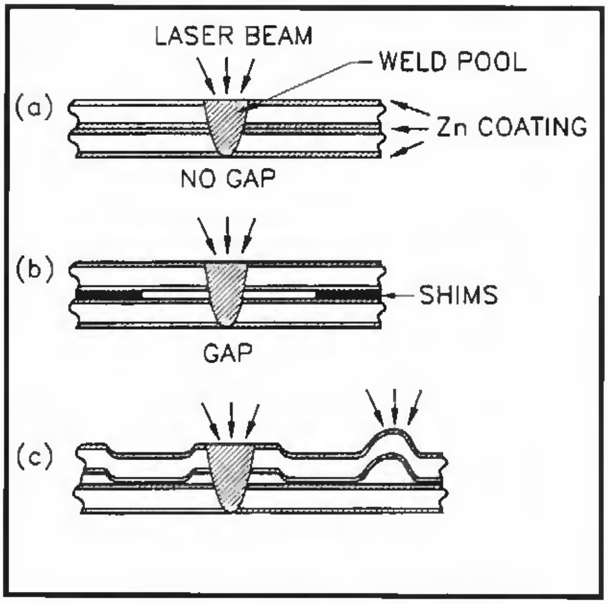

Fig. 1 — Schematic diagrams of weld joint geometries previously proposed for laser beam seam welding of coated sheet steels: A — No joint clearance between the sheets; B — a defined joint clearance between the sheets; C — defined joint clearances determined by prestamped projections in the top sheet.

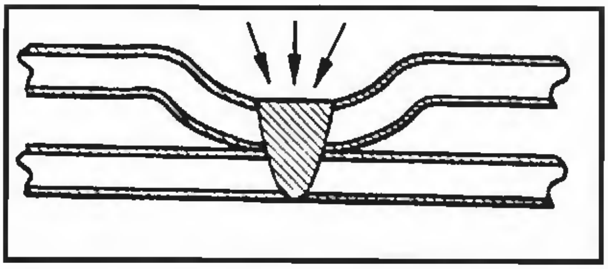

Fig. 2 — Schematic diagram of the groove-projection joint geometry used in this study for Nd:YAG laser beam seam welding of coated sheet steels.

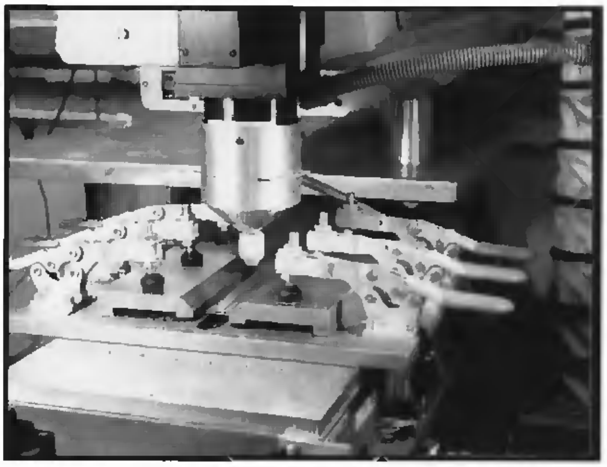

Fig. 3 — The clamping arrangement used for holding the weld specimens and the gas cup assembly of the JK702 pulsed Nd:YAG laser.

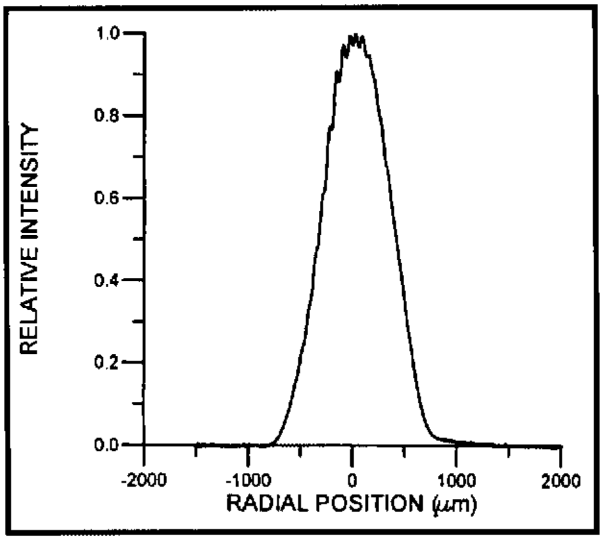

Fig. 4 — Representative power density distribution measured using a laser beam analyzer (LBA) at the focal position used in the experiments of the JK706 Nd:YAG laser when operating at 600-W output power and with a 160/160-mm lens combination.

ness ~8 µm), and 0.79-mm (0.03-in.) thick galvannealed sheet with a minimum coating of 40 g/m^2 (nominal coating thickness 6 µm). The compositions of the steel substrates are shown in Table 1.

The laser welding experiments were conducted using either 25 x 50-mm or 50 x 150-mm (1 x 2-in. or 2 x 6-in.) coupons of the coated sheet steels. To examine the effects on weld quality of the groove projection dimensions, grooves were pressed a predetermined depth into the top sheet of a specimen pair using either 0.99 or 1.40 mm (0.038 or 0.055 in.) diameter piano wires. The dimensions of the groove projections used in this study are listed in Table 2. Prior to welding, all specimens were ultrasonically cleaned in varsol and dipped in N-Heptane to remove dirt and oil. The two coupons of sheet steel were then clamped using the weld jig shown in Fig. 3 such that they were in contact only along the projection and welded along their line of contact as illustrated in Fig. 2.

The laser welding machines used for this study were a 250-W pulsed Nd:YAG laser (JK702), a 1-kW pulsed Nd:YAG laser (JK706), and a prototype 2-kW CW Nd:YAG laser (MW2000), all manufactured by Lumonics Corp. The JK702 pulsed laser had an adjustable beam expanding telescope (BET) and a 120-mm final focusing lens. The laser beams of the prototype MW2000 CW laser and the JK706 pulsed laser were transmitted to the workpiece through a 25- and 15-m long (82- and 49-ft), 1000-µm-diameter fiber-optic cable, respectively. Each beam was then recollimated by a lens as it exited the fiber and focused with a final process lens. The lens combinations for the MW2000 and JK706 lasers were: 160 and 80 mm; and 160 and 160 mm, respectively.

When using each laser, a preliminary set of welds was made to identify the optimum position of the beam focus relative to the groove surface on the basis of maximum penetration for a given laser power. This optimum position was different for each machine and is listed in Table 3. A laser beam analyzer (LBA) (Ref. 20) was used then to measure the spatial distribution of power density and the I/e^2 diameter of the laser beam at this operating position in the laser beam. The measured beams were multimode, but could be described approximately by a Gaussian distribution, as shown in Fig. 4. The I/e^2 beam diameters at the groove surface are listed also in Table 3.

In some welding trials using the prototype MW2000 laser and all of the welding trials performed with the JK702, the beam delivery system remained stationary and an x-y positioning table was used to move the workpiece at the desired rate. In other trials with the MW2000 laser and all experiments performed with the JK706 laser, the specimen to be welded was stationary and the fiber-optic beam delivery head was moved over the weld specimen using a Fanuc robot.

In the first and second series of experiments, the JK702 and JK706 pulsed lasers were used to explore the effects on weld quality of laser mean power, peak power and welding speed, and hence the amount of pulse overlap, when welding galvanized sheet steel with the series A groove-projection joint geometry-Table 2. In the first series of experiments with the JK702 laser, welds were made using a laser mean power of 220 W. This mean power was kept constant in order to prevent variation of the beam mode and diameter due to thermal lensing effects (Ref. 21). Various combinations of pulse energy and pulse time were obtained while using this constant mean power by varying the pulse frequency. For a particular welding condition (mean power, pulse energy, pulse time and frequency) the percentage of overlap between the pulse varied with welding speed. About 20 welds were made using an orthogonal matrix of experimental conditions in order to identify the pulse conditions that could be used to produce full penetration welds. The welding speeds used were 2.4, 3.6 and 4.8 mm/s, (5.6, 8.5 and 11.3 in/min) and pulse energies were varied from 31.9 to 38.3 J/pulse. Throughout these experiments, argon shielding was provided coaxially at a rate of 0.4 L/s (11.3 ft^3/h) through a 6-mm (0.24-in.) diameter orifice located 9 mm (0.35 in.) above the laser beam focal position.

In the second series of experiments, the JK706 pulsed laser with the fiber-optic delivery system was used to make 22 full joint penetration welds using a mean laser power of 720 W and a range of process conditions. The varied parameters included: energy/pulse, pulse time, focal position and welding speed. Argon shielding was provided through a 12.8-mm (0.5-in.) diameter back-jet located approximately 10 mm (0.04 in.) above the laser beam focal position at an inclined angle of 30 deg to the weld specimen.

In a third series of experiments, the prototype MW2000 CW laser was used to make about 30 welds under various process conditions in order to examine the weldability of the galvanized sheet steel with the series A and B groove-projection geometries — Table 2. Welding was performed at three mean powers: 685, 1000, and 1350 W using three to five welding speeds for each mean power. At 685 W, the three welding speeds were 5, 7.5 and 10 mm/s (11.8, 17.7 and 23.6 in./min); at 1000 W, the five welding speeds ranged from 15–30 mm/s (35.4-70.8 in./min); while at 1350 W, the five welding speeds ranged from 25-45 mm/s (59–106 in./min). In all

Table 1 — Composition (wt-%) of the 23-Ga Steel Sheet Substrates

Coating Type	C	Mn	P	S	Si	Al
Galvanized	0.03	0.24	0.010	0.011	<0.010	0.053
Galvannealed	0.03	0.25	0.007	0.015	0.025	0.073

Table 2 — Dimensions of Groove-Projection Geometries Used in This Study

Series	Wire Diameter (mm)	Groove Depth (mm)
A	1.40	0.70
B	0.99	0.50
C	1.40	0.35
D	1.40	0.24

cases, the welding speed was not increased further if incomplete joint penetration through the bottom sheet was observed. Argon shielding gas was provided coaxially at a rate of 0.4 L/s through a 3.2-mm (0.13-in.) diameter orifice located 3.5 mm (0.14 in.) above the laser beam focal position.

In the fourth series of experiments, the prototype MW2000 CW laser was used to explore the weldability of the galvanized and galvannealed sheet steel with all four groove-projection geometries listed in Table 2. Approximately 64 welds were made at two laser mean powers, 1200 and 1600 W, and using four welding speeds for each mean power. At 1200 W, the four welding speeds ranged from 27 to 43 mm/s (63.7–101.6 in./min), while at 1600 W, welding speeds ranged from 40 to 60 mm/s (94.5–141.7 in./min), where again, the welding speed was not increased if there was incomplete penetration of the bottom sheet. Argon shielding was provided in the same manner as described for the third series of experiments but was supplied at a rate of 0.23 L/s (6.5 ft^3/h).

The weld head geometry and weld quality of the laser welds produced were determined from transverse sections of the welds. A section of each seam weld was mounted in bakelite, then ground and diamond polished. Macro-etching was performed with a solution of picric acid (4 g in 100 mL methanol). Weld dimensions were measured using a metallographic microscope coupled to JAVA image analysis software. Finally, the failure mode and the load to failure were investigated by performing transverse shear tensile tests on an Instron tensile testing machine.

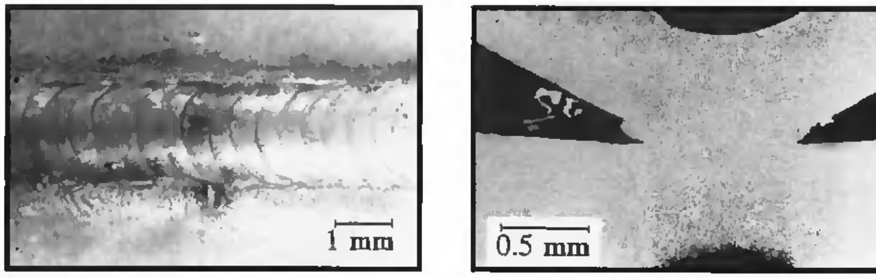

Fig. 5 — Weld produced in 23-ga galvanized sheet with series A groove-projection geometry using the JK702 pulsed laser at 220 W laser mean power with 34 J/pulse and a pulse time of 30 ms at 2.4 mm/s. A — Top view; B transverse section.

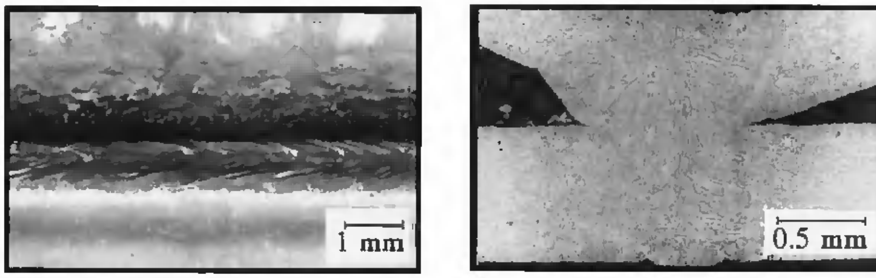

Fig. 6 — Weld produced in 23-ga galvanized sheet steel with series A groove-projection geometry using the prototype MW2000 CW laser at a laser mean power of 1350 W and a welding speed of 30 mm/s. A — Top view; B — transverse section.

Results and Discussion

Weld Quality

Good quality laser beam seam welds were produced in galvanized specimens with the series A groove-projection joint geometry using all three lasers. The acceptable welds produced with the JK702 and JK706 pulsed lasers displayed smooth top-bead surfaces with a fine rippled pattern generated by the successive overlapping laser pulses (Fig. 5A); whereas, the surface of the welds made with the prototype MW2000 CW laser displayed a centerline ridge running along the weld — Fig. 6A. As shown in

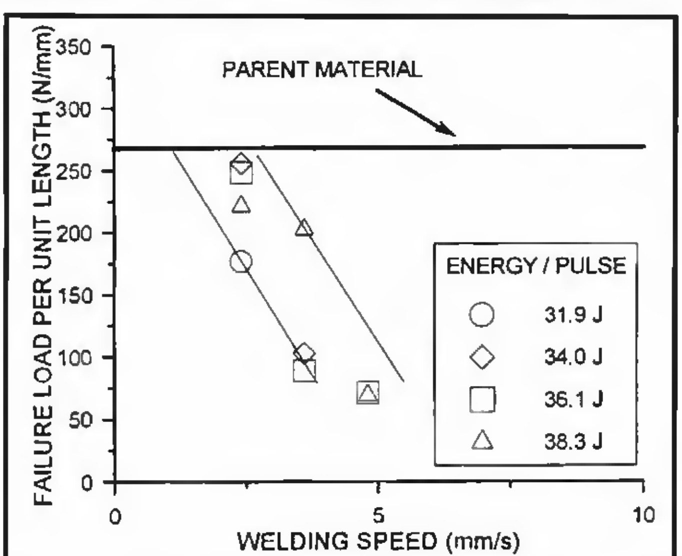

Fig. 7 — Transverse shear load to failure vs. welding speed of the laser beam welds produced in 23-ga galvanized sheet steel using groove-projection geometry A with the pulsed JK702 laser at a laser mean power of 220 W.

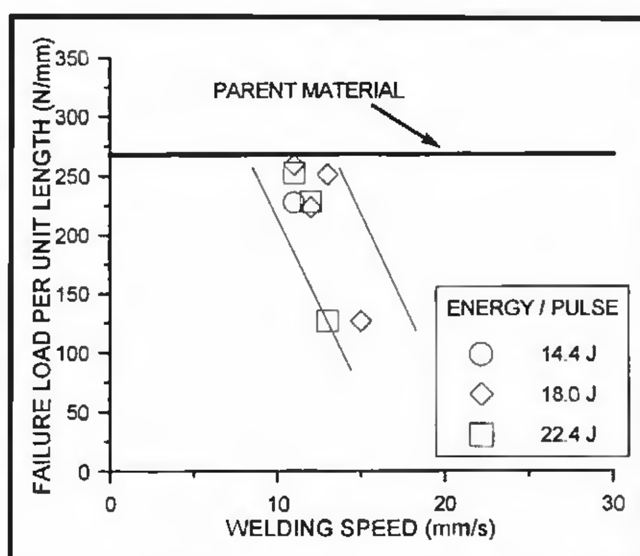

Fig. 8 — Transverse shear load to failure vs. welding speed of the laser beam welds produced in 23-ga galvanized sheet steel using series A groove-projection geometry with the pulsed JK706 laser at a laser mean power of 760 W.

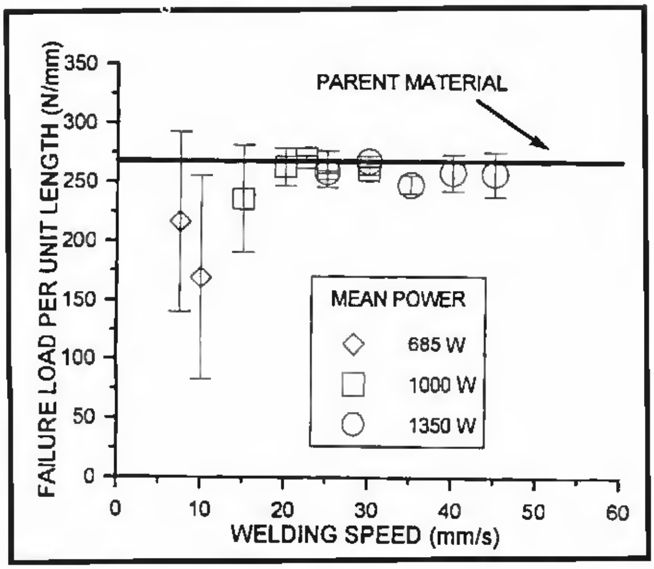

Fig. 9 — Transverse shear load to failure vs. welding speed of the laser beam welds produced in 23-ga galvanized sheet steel using series A groove-projection geometry with the MW2000 CW laser.

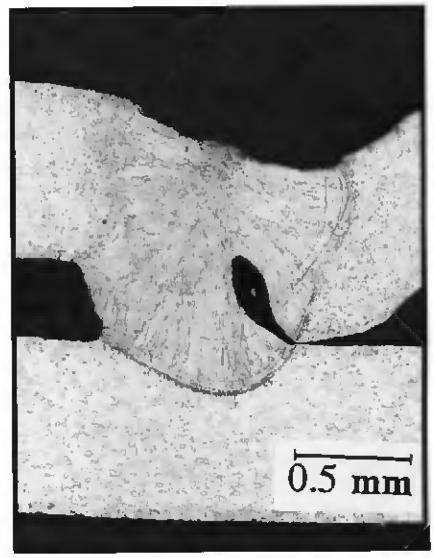

Fig. 10 — Tranverse section of a weld produced in 23-ga galvannealed sheet at 60 mm/s using 1600-W laser mean power and the series C groove-projection geometry. Note the porosity at the bottom of the groove due to inadequate venting of zinc vapor.

Figs. 5B and 6B, cross-sections of satisfactory welds fabricated with the pulsed and CW lasers were indistinguishable. These sections are typical of the acceptable welds. They are keyhole-mode welds that completely penetrate the second sheet of steel. There is no evidence of porosity at the interface generated by the vaporizing zinc layers, indicating that this groove-projection joint geometry has permitted adequate venting of the zinc vapors between the two sheets of steel during welding.

Welds displaying acceptable surface quality were made with the pulsed lasers over a limited range of processing conditions. The window of operating conditions which produced acceptable welds with the JK702 laser was concentrated at the upper limit of the laser's capabilities.

Table 3 — Optimum Location of the Laser Focal Position during Welding for Each Laser, and Resulting Laser Beam Diameter at the Groove Surface

Laser	Optimum Position of the Focused Laser Beam	$1/e^2$ Beam Diameter at Groove Surface (μm)
JK702	5.0 mm above Groove Surface	1570
JK706	Groove Surface	1200
MW2000	0.5 mm below Groove Surface	650
	1.0 mm below Groove Surface	740

Using the laser mean power of 220 W, good quality welds were produced at welding speeds ranging from 2.4 to 4.8 mm/s using laser pulse energies ranging from 31.9 to 38.3 J and pulse durations of 30 ms. The top surface of the welds produced at the lowest welding speed of 2.4 mm/s displayed pulse-to-pulse overlaps of approximately 75%. The backside of these welds showed continuous complete penetration or discontinuous penetration. The top surface of the welds produced at higher welding speeds displayed a lower amount of pulse-to-pulse overlap, while the backsides of the weld specimens generally did not show complete joint penetration. Welds fabricated at lower energies/pulse displayed inadequate penetration into the second sheet, while welds made at shorter pulse times suffered from blowholes, and in some cases, significant material loss. The tolerance box of acceptable processing conditions for welds made using the JK706 pulsed laser was centered about a pulse energy of 14.4–22.4 J/pulse with pulse times ranging from 2.5 to 2.8 ms. As in the case of the welds produced by the JK702 laser, the top surface of the welds produced at the lowest welding speed displayed a high percentage of pulse-to-pulse overlapping, on the order of 78 to 81%. The backside surface of these welds showed either continuous complete penetration or discontinuous penetration. As the welding speed increased, the amount of pulse-to-pulse overlap on the top surface decreased and the backside penetration showed reduced penetration.

Welds displaying good surface quality were made with the prototype MW2000 CW laser over a large range of laser mean powers and welding speeds. In general, acceptable quality welds were produced at laser mean powers of 1000 W or more and at speeds in excess of 20 mm/s. Complete joint penetration welds were produced when using 1600 W at speeds up to 47 mm/s, while partial joint penetration welds were successfully made at speeds up to 60 mm/s.

Weld Strength

The results of transverse shear tensile testing of the welds made using the JK702, JK706, and prototype MW2000 lasers are shown in Figs. 7, 8 and 9, respectively. For welds produced using the JK702 pulsed laser (Fig. 7), failure loads comparable to the base metal were observed for welds produced using the three highest energies/pulse and the lowest welding speed, 2.4 mm/s. Failure of these welded specimens always occurred in the base metal. It may be seen from this graph that the failure load per unit distance at a particular welding speed generally decreased with decreasing energy/pulse. The decrease in failure load per unit length seen with declining energies/pulse is also a consequence of reduced penetration into the second sheet. Also, the failure load decreased rapidly with increasing welding speed. Similarly, the decrease in failure load per unit distance with increasing welding speed can be attributed to reduced amounts of penetration of the second sheet due to lower amounts of pulse overlapping with increased welding speed. Similar trends were seen in the data obtained from the welds produced with the JK706 pulsed laser, as shown in Fig. 8. Once again, high failure loads with failure occurring in the base metal were associated with the highest energies/pulse at one welding speed, which in this case was 11 mm/s. This welding speed is more than four times greater than that possible with the JK702 pulsed laser.

The shear tensile strengths of the MW2000 CW laser welds are plotted vs. welding speed in Fig. 9. The welds made using laser mean powers of 1000 and 1350 W from the third series of experiments had failure loads comparable to the base metal and failed in the base metal. At the lowest laser mean power used, 685 W, and consequently, the lowest welding speeds, poor failure loads per unit distance were seen with failure occurring in the heat-affected zone or weld metal. These welds were characterized by wide top beads and poor penetration into the second sheet due to poor coupling of the laser beam with the workpiece at this laser mean power.

The transverse tensile shear strength and weld quality of all laser beam seam welds were adversely affected by misalignment of the laser beam with the centerline of the groove projection. An example of a transverse section through such a weld is shown in Fig. 10. In general, the surface quality of these welds was good and the misalignment of the laser beam on the surface of the workpiece was easily seen. However, this misalignment caused a reduction in the weld strength, and in most cases, a change in failure mode from failure in the base material to failure along the weld interface. Also, as may be seen in Fig. 10, misalignment of the laser beam sometimes caused intermittent weld metal porosity due to incomplete venting of the zinc vapor at the contact point between the bottom of the groove and the second sheet. In the extreme weld metal sagging or drop-through occurred, because the weld was created on the shoulder of the groove where the joint clearance was excessive. While experiments were not performed specifically to establish laser beam misalignment tolerance bands for successful welds with the groove geometry, examination of welds such as the one shown in Fig. 10 suggests that good welds should be produced provided the beam is within one beam radius of the groove centerline. For the weld in Fig. 10, which was produced using the MW2000 laser welding machine, the tolerance band would be about ± 350 μm (Table 3). Thus, these defects can be eliminated easily by minimizing laser beam misalignment using careful jigging or by using a joint tracker to follow the groove during welding.

Generally, the failure load and failure mode of welds that displayed acceptable surface quality could be predicted based on the degree of joint penetration evident on the backside of the workpiece. The shear tensile testing results indicated that welds which failed at relatively low strength levels, with failure occurring in the heat-affected zone or weld metal, showed varying degrees of heat marks consisting of resolidified zinc, but no areas of complete joint penetration on the backside of the workpiece. The welds which had some areas of complete joint penetration on the backside of the workpiece, even a small amount, such as shown in Fig. 11A, had failure loads comparable to the base metal, with failure occurring in the base metal. Failure also occurred in the base metal of welds which displayed more complete penetration,

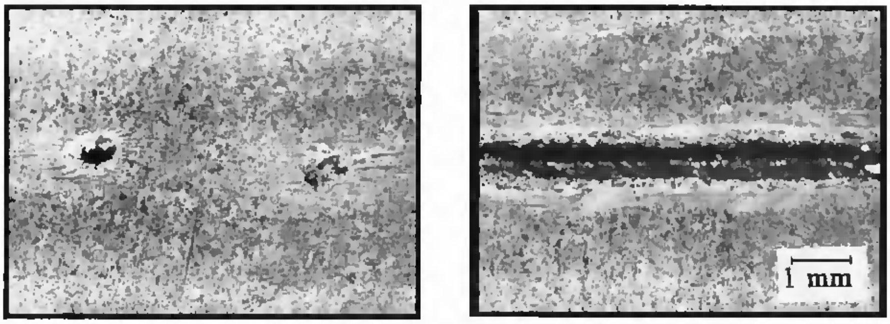

Fig. 11 — Views of the bottom surface of longitudinal welds produced in 23-ga galvanized sheet using series A groove-projection geometry which failed at levels comparable to the base metal. A — Backside of specimen displayed a few isolated areas of complete joint penetration; B — backside of specimen displaying continuous full joint penetration.

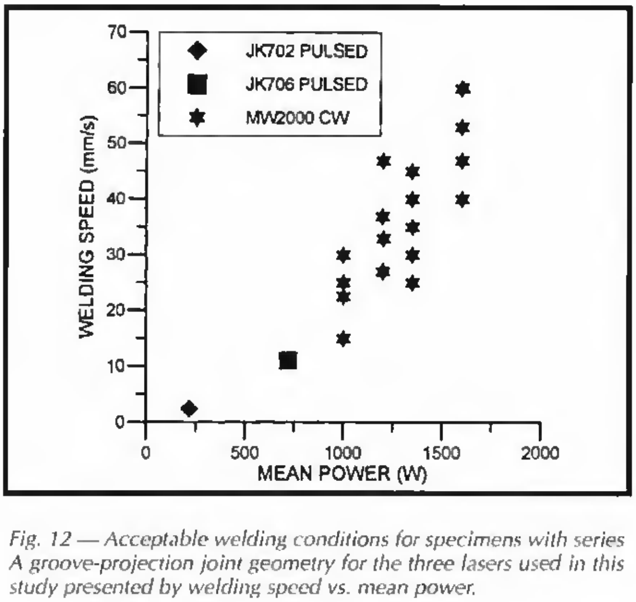

Fig. 12 — Acceptable welding conditions for specimens with series A groove-projection joint geometry for the three lasers used in this study presented by welding speed vs. mean power.

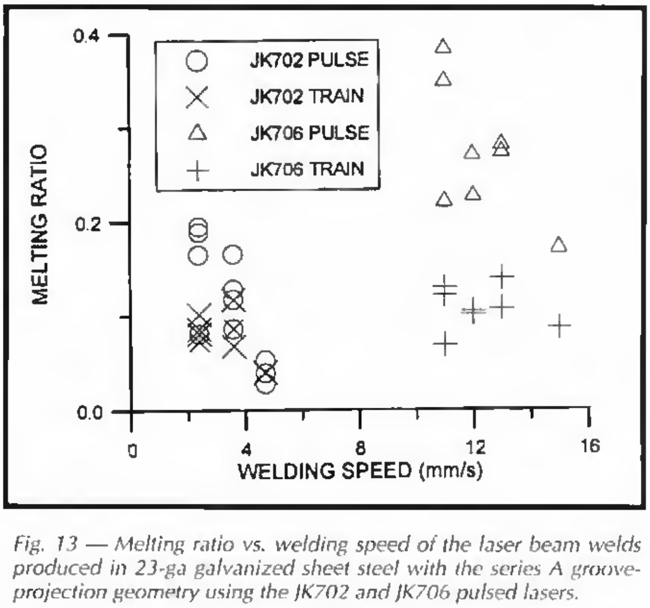

Fig. 13 — Melting ratio vs. welding speed of the laser beam welds produced in 23-ga galvanized sheet steel with the series A groove-projection geometry using the JK702 and JK706 pulsed lasers.

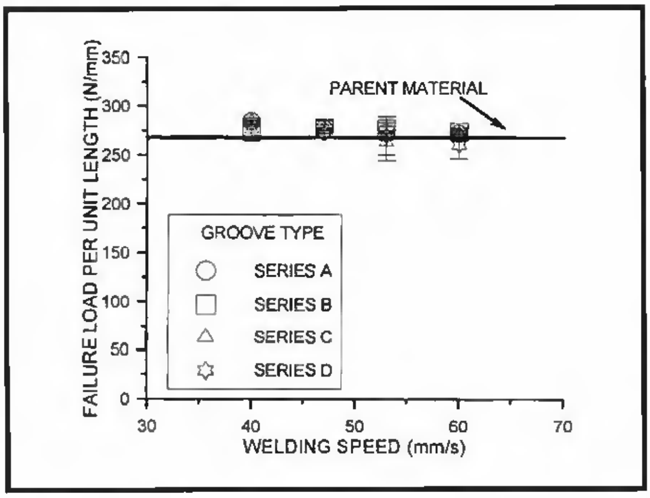

Fig. 14 — Melting ratio vs. welding speed of the laser beam welds produced in 23-ga galvanized sheet steel with the series A groove-projection geometry using the MW2000 CW laser.

such as shown in Fig. 11B.

The laser welding conditions resulting in good quality welds that failed at levels comparable to the base metal are plotted in Fig. 12 as a function of laser mean power and welding speed. These conditions were determined from a combination of qualitative evaluation of the weld surface quality and the shear tensile testing results. It can be seen from this graph that for each of the pulsed lasers acceptable quality welds were only produced at one welding speed. In contrast, good quality welds were fabricated over a large range of conditions with the prototype MW2000 CW laser. While this graph indicates a trend toward higher allowable welding speeds with increased available laser power, there will be a limit for this combination of material and laser beam diameter above which welds can be expected to become unacceptable due to the occurrence of humping and undercutting weld defects (Ref. 22). This limit was not reached in the present study.

Melting Ratio

The conversion efficiency of electrical energy to optical energy of most solid-state laser welding machines is typically less than 5%. However, when considering the overall welding process efficiency, it is usual to consider only the efficiency with which the output optical energy is used to form a fused joint. This effectiveness can be defined by either the melting efficiency or the melting ratio (Refs. 23, 24). The melting efficiency is defined as the ratio of energy required to heat and melt the weld metal to the energy absorbed by the workpiece; whereas, the melting ratio is defined as the ratio of energy required to heat and melt the weld metal compared to the output of the heat source, in this case, the measurable laser beam.

The melting efficiency of pulsed laser welding processes is difficult to determine because accurate measurements of the effective absorptivity are usually not possible. However, calculation of the melting ratio is possible because it requires only measurements of the laser beam energy and the volume of weld metal. In this study, therefore, the melting ratio was calculated for welds produced with the three different lasers to assess the relative effectiveness of each laser. The melting ratio, n_{mr}, is defined as

$$n_{mr} = \frac{V\left[\rho C_p\left(T_{mp} - T_0\right) + \Delta H_m\right]}{E} \tag{1}$$

where V is the melt volume (m^3), ρ is density (kg/m^3), C_p is the specific heat (kJ/kg-K), T_{mp} is the melting temperature (K), T_0 is the ambient temperature (K), ΔH_m is the latent heat of melting (kJ/kg) and E is the energy (J) of the laser pulse or beam. The thermophysical material properties used were those for AISI 1008 steel (Ref. 25).

Two different techniques were used to calculate the melting ratios of individual pulse welds vs. the melting ratios of a train of overlapping pulses or CW welds. For a single pulse weld, the volume of a single pulse weld was determined by measuring the boundary coordinates of the weld cross-section using a metallographic image analysis technique. Assuming that the weld pool was axisymmetric in shape, these boundary coordinates were then used to perform a numerical integration to provide the volume of weld metal. This value and the measured pulse energy used to produce the weld pool were then substituted into Equation 1 to calculate the melting ratio.

To determine the melting ratio for a train of pulses or a CW seam weld, the volume of weld metal produced per unit time was calculated by multiplying the welding speed by the cross-sectional area of the weld as measured using the metallographic image analysis technique. Assuming that the cross-sectional weld profile remained constant along the weld, this value for volume of weld metal produced per unit time and the energy input per unit time were used in Equation 1 to calculate the melting ratio.

The calculated melting ratios as a function of welding speed are shown in Figs. 13 and 14 for the pulsed lasers and CW laser, respectively. From the graph of results for the pulsed lasers (Fig. 13), it can be seen that the individual pulse melting ratios were as high as 0.4 and decreased with increasing welding speed for each laser. It may be expected that the melting ratio for the single pulse welds would be constant and independent of welding speed. The observed decrease of the melting ratio with increased welding speed may be due to an under estimation of the actual weld pool volume for welds

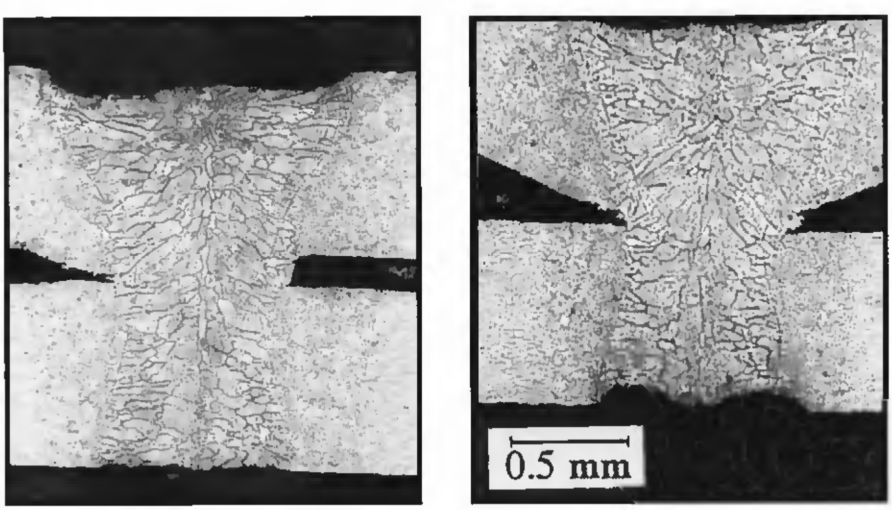

Fig. 15 — Transverse sections of longitudinal welds produced in 23-ga galvanized sheet using the MW2000 CW laser produced at a laser mean power of 1600 W at 40 mm/s with different series groove-projection geometries. A — Joint geometry D; B — joint geometry A.

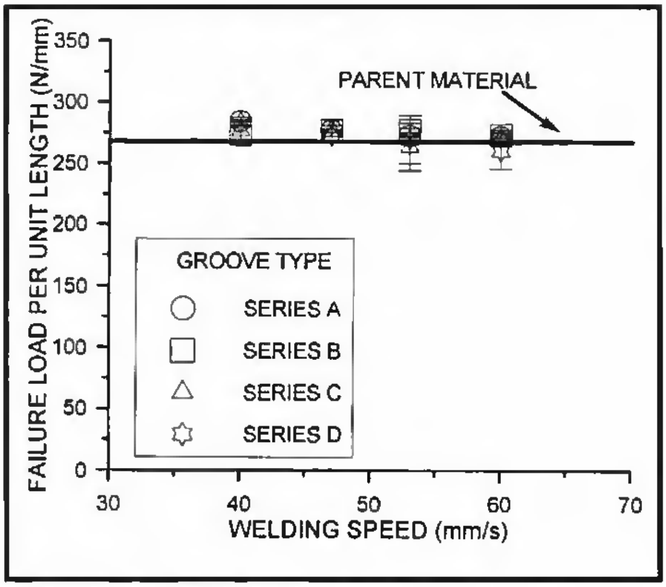

Fig. 16 — Transverse shear load to failure vs. welding speed of the laser beam welds produced on 23-ga galvanized sheet steel using the four different series of groove-projection geometries studied with the MW2000 CW laser at a mean power of 1600 W.

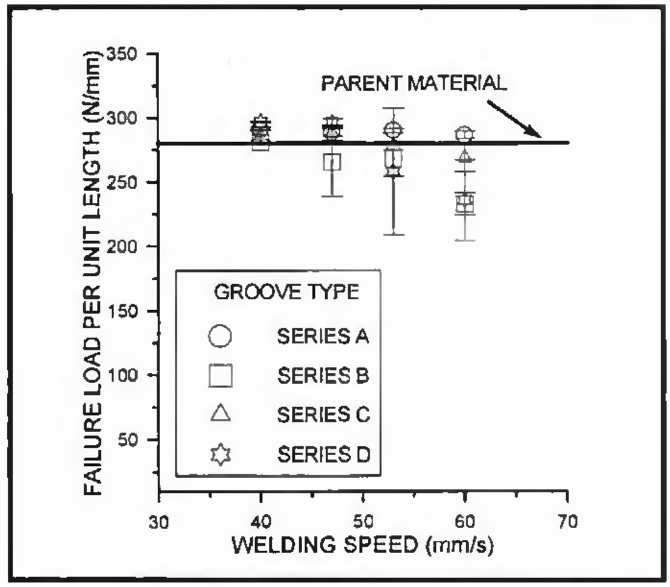

Fig. 17 — Transverse shear load to failure vs. welding speed of the laser beam welds produced in 23-ga galvannealed sheet steel using the four different series of groove-projection geometries studied with the MW2000 CW laser at a laser mean power of 1600 W.

produced at the higher speeds. As the welding speed increases, the weld pool width will decrease and the weld pool will become elongated in the direction of welding. Weld volume calculations based upon the weld cross-section and the assumption of an axisymmetric weld pool shape will, therefore, underestimate the actual weld pool volume, thereby causing a decrease in the calculated melting ratio as was observed.

In Fig. 13, the melting ratios of welds produced using pulse trains from both pulse lasers were approximately 0.1; that is, 10% of the laser beam energy actually contributed toward melting of the metal. Also, these values were always less than the melting ratios of the individual pulse welds at any given welding speed. This is because seam welds are produced using a pulsed laser by making a succession of overlapping individual spot welds. Thus, a portion of the weld metal is repeatedly reheated and melted, which inherently reduces the overall efficiency of the process. As the welding speed increased, the two types of melting ratios converged, because the amount of overlapping was reduced.

The melting ratios of welds produced using the prototype MW2000 CW laser are plotted as a function of welding speed in Fig. 14. The melting ratios of the good quality welds produced at 1000 and 1350 W from the third series of experiments had melting ratios of approximately 0.25 and did not vary significantly with welding speed. This melting ratio is 150% greater than the melting ratios calculated for the seam welds produced using the pulsed lasers. However, these melting ratios are still significantly less than the maximum theoretical melting efficiency of 48% for a CW complete joint penetration weld derived by Swift-Hook and Gick (Ref. 24). Finally, the melting ratios of welds from the third series of experiments, which were produced at 685 W and previously deemed unacceptable, had much lower melting ratios which were comparable to the melting ratios of trains of pulses from the two pulsed lasers. This is consistent with the previous observations of poor weld quality and incomplete penetration in welds produced using this lower power.

Effect of Groove Size and Coating Type

Good quality welds were produced with the prototype MW2000 CW laser in both galvanized and galvannealed welded specimens and with all four groove-projection geometries used (see Series A-D in Table 2). As illustrated by the representative transverse sections of welds produced using a large and a small groove depth in Fig. 15, weld quality, size and shape were not significantly affected by the variations in groove dimensions used in this study. The results were also independent of coating type.

The results from the transverse shear tensile tests of galvanized and galvannealed specimens made with the four different groove geometries from the fourth series of experiments at a laser mean power of 1600 W are shown in Figs. 16 and 17, respectively. From these graphs, it can be seen that all of the welds produced with both the galvanized and the galvannealed specimens failed at levels comparable to the base metal with failure occurring in the base metal. With the galvanized material, no significant variation in strength was seen for the welds produced with different groove sizes. However, results from the galvannealed specimens showed more variation of failure load per unit length as a function of the groove sizes, especially at high welding speeds.

Summary

The weldability of coated sheet steels when using a modified lap joint geometry consisting of a rounded groove-shaped projection pressed into the top sheet of the specimen pair has been investigated by making seam welds using a wide range of process conditions with three different Nd:YAG lasers: a 250-W pulsed laser, a 1-kW pulsed laser with a fiber-optic delivery system and a prototype 2-kW CW laser with fiber-optic delivery system.

Good quality welds were produced in 0.75-mm-thick (23-gauge) galvanized sheet steel with the two pulsed lasers under a limited set of process conditions and with the 2 kW CW laser over a wider range of process conditions. The top surface features of the welds depended on the output waveform (pulsed vs. CW), but transverse sections of the good welds displayed no discernable differences.

The transverse shear tensile strength of acceptable welds produced with all three lasers was comparable to the base metal strength. However, the strength of the laser beam welds were adversely affected by laser beam misalignment with the groove projection centerline, or incomplete penetration through the second sheet of steel.

The welding speeds that produced acceptable quality welds increased with laser power. The fastest speeds that produced good quality welds in the 23-ga coated sheet steels were 2.4 mm/s with the 250-W pulsed laser, 11 mm/s with the 1-kW pulsed laser and 60 mm/s with the prototype 2-kW CW laser. The melting ratios were approximately 0.1 in seam welds produced using the pulsed lasers but were about 0.25 in welds produced using the CW laser. Thus, the overall process efficiency was about 150% greater when using a CW laser compared to a pulsed laser. Finally, unlike previous controlled joint clearance techniques, weld quality of laser welds made with the new groove-projection lap joint configuration was not found to be sensitive to the groove dimensions, the type of coating or variations in coating thickness.

Acknowledgments

This work was supported by the Ontario Center for Materials Research (OCMR) and the Ford Motor Co. Lumonics Corp. graciously provided the use of their high-power prototype Nd:YAG laser facilities. The contributions of H. N. Bransch formerly of Lumonics Corp. during the welding experiments and S. Hong during metallurgical evaluation of the laser welds are gratefully acknowledged.

References

1. Heyden, J., Nilsson, K., and Magnusson, C. 1988. Laser welding of zinc coated steel. *Lasers in Manufacturing*, ed. H. Hugel, pp. 93–104. Cotswold Press Ltd, Oxford, U.K.

2. Heyden, J., Nilsson, K., and Magnusson, C. 1990. Laser welding of zinc coated steel. *The Industrial Laser Annual Handbook*, 1990 Edition. Eds: D. Belforte and M. Levitt, pp. 161–167, Penn Well Books, Tulsa, Oka.

3. Kennedy, S. C., and Norris, I. M. 1989. Nd:YAG laser welding of bare and galvanized steels. *Intl. Congress and Exposition*, Detroit, Mich., SAE Technical Paper 890887.

4. Berlinger, G., and Speranza, J. J. 1987. Laser Welding Metal Sheets with Associated Trapped Gases. U.S. Patent No. 4,684,779.

5. Washio, K. 1992. Welding and cutting of car-body metal sheets with Nd:YAG lasers by flexible fiber beam delivery. *Sheet Metal Welding Conf. V.* AWS Detroit section. Detroit, Mich.

6. Aruga, S., Matsui, E., Okino, K., Takenaka, H., Sato, K., Kyusho, Y., and Washio, K. 1992. Efficient and high-quality overlap welding of car-body aluminum alloy and sheets with high power Nd:YAG laser by flexible beam delivery. *Proc. Laser Advanced Materials Processing*, LAMP '92, pp. 517–522. Nagaoka, Japan. Japan High Temperature Soc.

7. Washio, K., Takenaka, H., Okino, K., Aruga, S., Matsui, E., and Kyusho, Y. 1992. Welding and cutting car-body metal sheets with fiber delivered output from high-power Nd:YAG lasers. NEC Research and Development, NEC Corp. 33 (1): 102–109.

8. Graham, M. P, Hirak, D. M., Kerr, H. W., Weckman, D. C. 1994. Nd:YAG laser welding of coated sheet steels. *Journal of Laser Applications*.

9. Williams, S. W., Salter, P. L., Scott, G., and Harris, S. J. 1993. New welding process for galvanized steel. *Proc. 26th Intl. Symp. Automotive Technology & Automation*. Aachen, Germany, pp. 49–56.

10. Pennington, E. J. 1987. Laser Welding of Galvanized Steel. U.S. Patent No. 4,642,446.

11. Rito, N., Ohta, M., Yamada, T., Gotoh, J., and Kitagawa, T. 1988. Laser Welding Method. U.S. Patent No. 4,745,257.

12. Aknter, R., Steen, W. M., and Cruciani, D. 1988. Laser welding of zinc coated steel. *Lasers in Manufacturing*, ed. H. Hugel, pp. 195–206. Cotswold Press Ltd., Oxford, U.K.

13. Akhter, R., and Steen, W. M. 1990. The gap model for welding zinc coated steel sheet, *Proc. Intl. Conf. Laser Systems Application in Industry*. pp. 219–236. Assoc. Tecnica del' Automobile, Italy.

14. Imhoff, R., Behler, K., Gatzweiler, W.,and Beyer, E. 1988. Laser beam welding in car body making. *Lasers in Manufacturing*. ed. H. Hugel, pp. 247–258. Cotswold Press Ltd, Oxford, UK.

15. Bagger, C., Miyamoto, I., Olsen, F., and Maruo, H. June, 1992. Process behaviour during high power CO_2 laser welding of zinc coated steel. *Proc. Laser Advanced Materials Processing LAMP '92*. eds. A. Matsunawa and S. Katayama, pp. 553-558. Nagaoka, Japan. Japan High Temperature Society.

16. Hanicke, L., and Strandberg, O. 1993. Roof laser welding in series production. *SAE Intl. Congress and Exposition*. Detroit, Mich, SAE Technical Paper 930028.

17. Petrick, F. D. 1990. Method of Making Hemmed Joints Utilizing Laser Welding. U.S. Patent No. 4,916,284.

18. Piane, A. D., Sartorio, F., Cantello, M. and Ghiringhello, G. 1987. Method of Laser Welding Sheet Metal Protected by Low-Vaporizing-Temperature Materials. U.S. Patent No. 4,682,002.

19. Spies, B., and Thoms, V. 1992. Welded Lap or Web Joints for Galvanized Sheet. U.S. Patent No. 5,104,032.

20. Hirak, D. M., Weckman D. C., and Kerr, H. W. 1994, measuring the spatial intensity distribution of high power focussed laser beam analyses, *Meaure Sci & Techn*; Vol. 5 pp 1513-1532

21. Bransch, H. N., Weckinan, D. C., and Kerr, H. W. 1994. Effects of pulse shaping on Nd:YAG spot welds in austenitic stainless steel. *Welding Journal* 73(6): 141-s to 151-s.

22. Albright, C. E., and Chiang, S. 1988. High-speed laser welding discontinuities. *Journal of Laser Applications* 1(1): 18–24.

23. Fuerschbach, P. W. 1992. Melting efficiency in fusion welding. *The Metal Science of Joining*. eds. M. J. Cieslak, J. H. Perepezko, S. Kang, and M. E. Glicksman, pp. 21–29. TMS-MME, Warendale, Pa.

24. Swift-Hook, D. T., and Gick, A. E. F. 1973. Penetration welding with lasers. *Welding Journal* 52 (11): 492-s to 499-s.

25. Pehlke, R. D., Jeyarajan, A., and Wada, H. 1992. NTIS Report No. NSF-MEA-82028. University of Michigan, Ann Arbor, Mich.